Composites Communications 53 (2025) 102254

Contents lists available at ScienceDirect

Composites Communications

journal homepage: www.elsevier.com/locate/coco

Compression, impact and residual strength after impact properties of graphene/fiberglass/epoxy multiscale composites

M. Rafiee [a,*], A. Fallah [b], S. Hosseini Rad [c], M.R. Labrosse [a]

[a] Department of Mechanical Engineering, University of Ottawa, Ottawa, ON K1N 6N5, Canada
[b] Department of Mechanical Engineering, Iran University of Science and Technology, Tehran, Iran
[c] Department of Mechanical Engineering, Polytechnique Montreal, Montreal, QC H3T 1J4, Canada

ARTICLE INFO

Keywords:
Compression
Impact strength
Residual strength after impact
Fiberglass/epoxy composites
Nanomaterials

ABSTRACT

The effect of graphene nanoplatelets (GNPs), graphene oxide (GO), and reduced-graphene oxide (rGO) on compression, impact and residual strength after impact properties of glass-fiber reinforced polymer composites (GFRPs) were examined. Vacuum-assisted resin transfer molding (VARTM) method was used to simultaneously modify the fibers and the matrix with carbon nanomaterials. A solution of nanoparticle/epoxy mixed in a solvent was sprayed onto the fabric and was also introduced into the epoxy matrix by an agitator mixer. The results from tensile testing indicated that the addition of GNPs, GO, and rGO augmented the mechanical properties of glass fiber-reinforced composites. According to our experimental results, both fiber and matrix-dominant properties were improved under compression, impact and residual strength after impact properties tests, leading to a superior composite.

1. Introduction

The requirements for the development of high strength and low weight epoxy composite materials have increased continuously for application in the automobile and aerospace industries, etc. [1,2]. Studying compression, low velocity impact and residual strength after impact (also known as post-impact strength or compression after impact strength) is significant for the structural aspect of vehicles to protect them from damage. Hence, considerable research (e.g. Refs. [3,4]) has been carried out to evaluate the strength of the reinforced epoxy polymers under different types of compressive loading lately.

In recent years, significant efforts have been spent to improve compression, low velocity impact and residual strength after impact behavior of fiber reinforced epoxy composites. Among them, the inclusion of nanoscale particles incorporation into the epoxy matrices has offered a variety of new possibilities in this area [5–7]. Recently, derivatives of graphite such as graphene nanoplatelets (GNPs) and graphene oxide (GO) have been investigated due to their 2D layered structure combinations leading to high thermal, mechanical and electrical properties [8–11]. Many researchers have investigated the graphene-related polymer matrix composites [12–14]. Shanmugam et al. [15] investigated the influence of graphene on hybrid (flax/E-glass/epoxy) fiber-reinforced polymer (HFRP) composites at diverse compositions. They demonstrated that adding 0.6 wt% of graphene to HFRP composite laminates enhanced the strength of composites outstandingly. Çakır et al. [16] examined the effect of various compositions of graphene nanoparticles on the flexural and shear behaviors of glass fiber-reinforced polymer plates (GFRP) adhesively bonded joints were investigated. According to their results, 0.3 wt% graphene nanoparticles improved shear strength by 145 %. Moreover, adding 0.2 wt% of graphene nanoparticles showed a 100 % increase in flexural strength.

While improving the compressive strength, low-velocity impact resistance, and residual strength after impact is of paramount importance for high-performance composite materials, little work has directly addressed these properties in graphene/glass fiber/epoxy nanocomposites. Nash et al. [17] provided a comprehensive overview of toughening methodologies (bulk matrix toughening and inter-/intralaminar toughening), suitable materials, and their effects on the impact and post-impact behavior. Dogan et al. [18] investigated the effect of GNPs inclusion on mechanical (tensile and flexural) and low-velocity impact characteristics of carbon and glass fiber-reinforced hybrid composites. The authors showed that the incorporation of GNPs at certain concentrations affects the impact resistance and

* Corresponding author.
E-mail addresses: mrafiee@uottawa.ca, mrafiee20@gmail.com (M. Rafiee).

https://doi.org/10.1016/j.coco.2025.102254
Received 29 July 2024; Received in revised form 21 December 2024; Accepted 2 January 2025
Available online 3 January 2025
2452-2139/© 2025 The Authors. Published by Elsevier Ltd. This is an open access article under the CC BY license (http://creativecommons.org/licenses/by/4.0/).

mechanical properties of carbon/glass fiber-reinforced hybrid composites significantly. In another study [19], they demonstrated the addition of 0.25 wt% GNPs into the epoxy matrix increased the low-velocity impact (LVI) properties of hybrid fiber-reinforced composites and pure glass. To improve the low-velocity impact characterization of the composites, Rahman et al. [20] added nanoclay and GNPs into Kevlar fiber-reinforced Epoxy composites. The fillers were added up to 10 wt% with 16 ply Kevlar epoxy composites. It was found that the nanoclay was more effective than graphene for impact resistance and the absorption of impact energy. Rezvani Tavakol et al. [21] investigated the influence of graphene nanoplatelets on a novel foam-based sandwich panel structure. They demonstrated that adding 0.3 % nano to the sandwich structure displayed more stable behavior in impact resistance and energy absorption than other samples. Vigneshwaran et al. [22] demonstrated that adding 1 wt% GNPs to both fiber and matrix enhanced impact resistance by 45 % and tensile strength by 114 %. Demirci [23] investigated the effect of GNPs on the low-velocity impact behaviors of the basalt fiber reinforcement (BFR) laminated face sheets. It was demonstrated that GNPs raised the impact resistance of BFR/aluminum honeycomb composite sandwich structure as well as confined and decreased damage development. Fathi et al. [24] examined the effect of graphene nanoplatelets on the low-velocity impact (LVI) behavior of composites and FMLs (fiber metal laminates). Their results showed that 0.2 wt% of GNPs reinforced the impact resistance of FMLs. The outcomes of these studies highlight the significant improvements achieved through the incorporation of carbon and other nanomaterials into fiber-reinforced composites. For instance, enhancements in mechanical properties such as flexural, tensile, and impact strength were demonstrated, with up to 145 % improvement in shear strength and 114 % increase in tensile strength achieved by optimizing nanoparticle compositions. These findings underline the potential of graphene derivatives for advancing composite material performance by tailoring properties to meet demanding structural requirements.

The aim of this research is to investigate the addition of graphene derivative nanoparticles into the matrix of polymeric composites to enhance compressive strength, low-velocity impact resistance, and residual strength after impact in multiscale composites. While considerable progress has been made in improving these properties in various types of composite materials, such as hybrid fiber-reinforced polymers, foam-based sandwich structures, and fiber metal laminates, limited studies focus specifically on graphene/glass fiber/epoxy nanocomposites under compressive and post-impact loading conditions. In this study, the addition of graphene derivatives nanoparticles into the matrix of polymeric composites was studied to improve the compressive, low-velocity impact, and residual strength after the impact of multiscale composites. The VARTM method was used for the processing of laminates.

2. Experimental

2.1. Materials

Graphene oxide was purchased from Ablalonyx, Norway and through its thermal reduction, reduced-graphene oxide (rGO) was produced. Non-functionalized GNPs with a mean thickness of 1.5 nm and diameter of 5 μm were provided from Cheap Tubes Inc., U.S.A, glass fibers (unidirectional E-glass) with average diameter of 20 μm were purchased from NMG, China. The diethyltoluenediamine (DETDA) curing agent PT-2712 Part B1 and diglycidyl ether of bisphenol-A (DGEBA) epoxy resin PT-2712 Part A were sourced from PTM&W Industries, Inc., USA. As per manufacturer recommendation, mixing weight ratio of epoxy resin Parts A and B was 100:22.

2.2. Preparation of multi-scale nanocomposites

The GFRP nanocomposites reinforced with GNPs and rGO were prepared with different loading percentage of nanoparticles as described in Table 1 [25,26]. Nanoparticles were added into the composites in two steps, first for sizing the fabrics and second for reinforcement of the matrix. E-Glass unidirectional fabrics with weight per area of 1200 g/m2 were used in this study. Table 2 shows the loading of nanoparticles for each step. To allow for an efficient dispersion of nanoparticles, acetone was chosen as it has been reported to have a satisfactory result due to its proper boiling point [1] and no negative effect on pre-curing process [27]

Dispersion of nanoparticles in acetone (1 g/L) was performed by sonication using an ultrasonic probe (Q700 Sonicator, Qsonica LLC, USA) for 90 min, 20-sec ON pulses followed by 10-sec OFF cycles for controlling the temperature. The sizing of the fibers using a spray gun with the desired amount of mixture (14 g/ft^2 of both sides of fabric) was performed inside a fume hood, following 24 h rest to ensure full evaporation of the solvent.

The rest of the solution was stirred at 400 rpm for 12 h to achieve a proper dispersion state. For the solvent to eveporate, the mixture was mixed with magnetic stirrer for 4 h at 70 °C followed by drying in a vacuum chamber for 30 min to complete the solvent elimination. To control premature curing, the resin and curing agents were mixed at room temperature with a hardener (low viscosity DETDA) to epoxy ratio of 22:100. Using a mechanical stirrer, the solution was mixed at 800 rpm for 30 min and degassed under vacuum at room temperature for about 30 min. The final solution was then used as an infusion resin for the fabrication of the nanocomposites.

The composites were fabricated with the nanomaterial-modified resin through the VARTM method [25]. Fiberglass fabrics (three layers) in cross ply form (0°,90°,0°) was used, where 0° was the main direction of testing. Curing of infused nanomaterial/epoxy composites at ambient temperature for 15 h was followed by a post cure rate of 1 °C/min, held every 20 °C for an hour. Final step was resting samples at 100 °C 3 h to eliminate any possible thermal history.

Samples were then cut into the desired size (1.9 ± 0.1 mm in thickness) by waterjet. Fiber volume and weight fraction percentages were calculated according to ASTM D3171 and found to be 50 % and 70 %, respectively. The material properties of each material used in the fabrication of the multi-scale composites are given in Ref. [25]. More details regarding the process flow and material structure of the developed composites are given in Ref. [25].

3. Characterization

3.1. Compression

All compression tests were performed on a universal testing machine (Instron 4482) according to ASTM D6641 to obtain the compressive young modulus, compressive strength and ultimate strain of the test coupons at room temperature. The specimen dimensions were 140 mm × 13 mm with gauge length of 13 mm. Five coupons per panel were

Table 1
Concentration of additives used for reinforcement of composites.

	wt% of DGEBA	vol% of DGEBA	wt.% of matrix (DGEBA + DETDA)	vol% of matrix (DGEBA + DETDA)	wt.% of total (DGEBA + DETDA + fibers)	vol% of total (DGEBA + DETDA + fibers)
GNP	0.1	0.55	0.08	0.44	0.02	0.22
	0.2	1.1	0.16	0.88	0.05	0.44
	0.4	2.2	0.33	1.76	0.1	0.88
	1	5.5	0.82	4.4	0.25	2.2
rGO	0.01	1.1	0.008	0.88	0.002	0.44
	0.03	3.3	0.025	2.64	0.007	1.32
	0.042	4.6	0.034	3.7	0.010	1.85

Table 2
Amount of nanoparticle used for sizing and infusion of fiberglass/epoxy composites.

	wt.% of DGEBA	vol% of DGEBA	Sprayed vol. %	Infusion vol%
GNP	0.1	0.55	0.275	0.275
	0.2	1.1	0.55	0.55
	0.4	2.2	1.1	1.1
	1	5.5	4.4	1.1
rGO	0.01	1.1	0.55	0.55
	0.03	3.3	2.2	1.1
	0.042	4.6	3.5	1.1

tested for each mechanical testing. The testing coupons were loaded at a constant crosshead speed of 1.3 mm/min.

3.2. Impact

The impact tests were conducted using an Instron Dynatup 8200 instrumented drop-weight impact tower equipped with a hemispherical tip, which follows the ASTM D7136 standard. In this test, a 0.625-in diameter hemispherical drop weight impactor weighing 6.143 kg was used to impact the rectangular 100 (width)mm × 150 (length) mm test sample by dropping it from an Instron Dynatup 8250 drop weight impact test tower. The potential energy of the impactor (as calculated from the weight and drop height) was 37 J.

3.3. Residual strength after impact

The compression after impact (CAI) tests of the impacted nanocomposites were fulfilled on a universal testing machine according to ASTMD7137 standard. The CAI testing speed was 1.3 mm min $^{-1}$. CAI fixture was based on ASTM D7137 due to the thinness of the composite sample. The samples were clamped at the bottom edge and two sides to avoid buckling during compression. The CAI tests were conducted at room temperature (23 °C, relative humidity 50 %). The compression load was applied to the samples after they were damaged under low velocity impact load. Test repetition was carried out for three samples of each material.

4. Results and discussion

4.1. Morphology

The morphology of fiber on the fracture surface of fiberglass/epoxy composites was observed to investigate the quality of interfacial bonding. In Fig. 1a, a glass fiber was pulled out from the neat epoxy matrix and very little epoxy resin matrix remained on the surface of the fiber. The edge of holes left by the fiber pullout was round and the sidewall was smooth, indicating that stresses did not uniformly transfer between carbon fibers and the resin matrix under tensile load. By contrast, in Fig. 1b, it can be observed that there were no gaps between the graphene-coated glass fibers and the epoxy matrix containing nanoparticle reinforcements, suggesting a strong interfacial bound between fibers and matrix. The more cohesive structure could help to increase the absorption of rupture energy and achieve an effective load transfer between fiber and polymer matrix. The edges of holes were irregular and the sidewalls were rough, indicating the destruction of the resin matrix around the fibers due to the improved interfacial cohesion after adding the nanoparticle reinforcements.

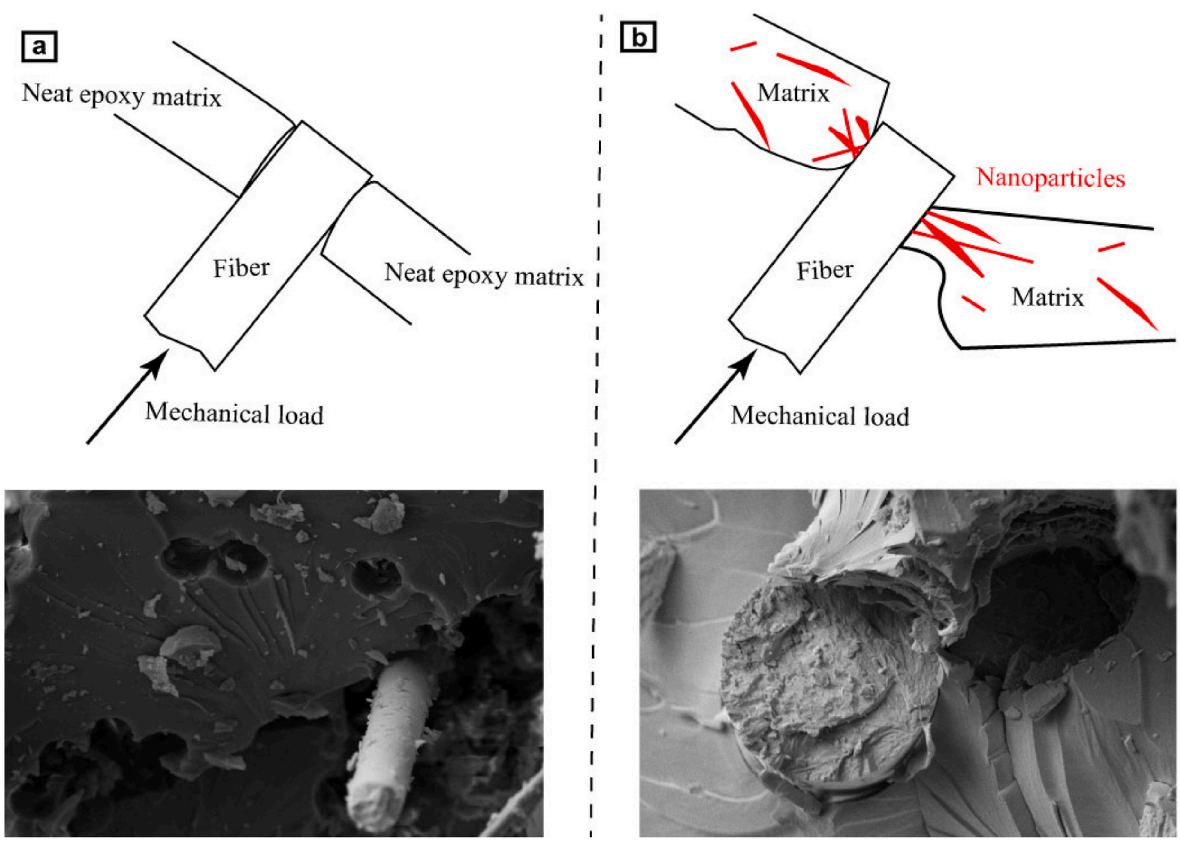

Fig. 1. SEM images of the failure surface with the hole left by the fiber pullout in composite specimens: (a) the fractured conventional glass fiber/neat epoxy composites; (b) the fractured nanoparticle-sized glass fiber in the nanocomposite epoxy composites; The top inset is simplified model for the anchoring effect of nanoparticle reinforcements at interface under load.

4.2. Compression

The compression stress-strain curves for the baseline neat glass–epoxy composite as well as graphene-modified glass–epoxy composite for all samples tested are shown in Fig. 2. Compressive modulus, ultimate strain and ultimate strength values are plotted in Table 3. As can be seen from Fig. 2., for all configurations containing GO and rGO, the measured compressive strength was higher than the baseline values. However, in the case of GNPs, adding 0.1 wt% of GNPs improved the compressive strength, but a further increase in GNPs reduced the compressive properties. Agglomeration of graphene layers at higher contents is expected to be the reason for a decrease in compressive performance of GNPs-modified composites. GNP agglomerates can cause cracks to initiate and propagate and thus decrease the strength of the composites.

Some numerical values corresponding to the compressive behavior of sample extracted from Fig. 2 are also shown in Table 3. For instance, adding 1 and 2 wt% graphene oxide (GO) to the composite improved the compressive modulus of the baseline panel by 16.4 % and 16.7 %, respectively. Similarly, the inclusion of reduced graphene oxides (rGOs) increased the compressive modulus of the baseline composite by 12.3 %, 6.9 %, and 14.1 % for the incorporation of 0.01, 0.03, and 0.042 wt%, respectively. These improvements in compressive modulus are attributed to the reduction in delamination of the composites due to the strong interfacial bonding between the epoxy matrix and graphene nanomaterials.

However, not all loadings of graphene nanoplatelets (GNPs) resulted in improved performance. Experimental results indicate that the addition of 0.1 wt% GNPs led to a modest 4.9 % improvement in compressive modulus, while further increases in GNP loading failed to provide additional enhancements. This aligns with previously published studies on graphene-based materials, such as [28].

The improvement in compressive behavior can be further explained by analyzing the failure evolution in these composites. The presence of graphene nanomaterials contributes to enhancing the interfacial bonding, which delays the onset and propagation of micro-cracks and delamination during compressive loading. This improved crack resistance likely leads to the observed increases in compressive modulus at certain loadings. However, at higher GNP concentrations, agglomeration of nanoparticles may occur, creating localized stress concentrations that counteract the benefits of graphene reinforcement. Additionally, excessive GNP loading can disrupt the uniformity of the resin matrix, leading to premature failure modes such as buckling or matrix cracking.

To provide a more comprehensive understanding of the mechanisms involved, future studies should incorporate detailed analyses of the failure evolution under compressive loads. Techniques such as scanning electron microscopy (SEM) and digital image correlation (DIC) could help visualize crack initiation and propagation, delamination, and fiber-matrix interactions. Such insights would contribute to establishing the optimal nanoparticle loading and reinforcing mechanisms for achieving superior compressive performance in glass fiber/epoxy composites.

Table 3
Compressive modulus, maximum compressive strength and maximum compressive strength of nanocomposites containing (i) GO, (ii) rGO and (iii) GNPs.

Case	Compressive modulus (GPa)		Ultimate compressive strain		Ultimate compressive strength (MPa)	
	Average	STD Dev.	Average	STD Dev.	Average	STD Dev.
Neat Epoxy	21.9	1.3	0.014	0.002	226.1	14.1
GO 1 %	26.2	2.7	0.013	0.001	247.9	20.8
GO 2 %	24.2	1.3	0.013	0.000	234.3	20.6
rGO 0.01 %	24.1	1.8	0.013	0.001	235.1	9.0
rGO 0.03 %	23.1	1.2	0.016	0.006	224.2	10.2
rGO 0.042 %	25.1	2.4	0.014	0.002	247.0	7.3
GNPs 0.1 %	22.4	0.5	0.016	0.003	246.8	11.5
GNPs 0.2 %	20.9	0.9	0.014	0.001	217.2	6.4
GNPs 0.4 %	20.7	0.2	0.015	0.000	221.6	14.3
GNPs 1.0 %	20.8	1.2	0.014	0.002	216.4	4.9

The trend for ultimate strain appeared to be different from the corresponding compressive modulus. Overall, the addition of graphene nanoparticles seemed to result in fairly lower elongation in the test coupons. This might be due to the introduction of potential voids and microcracks, and therefore stress concentrations developed by introducing nanoparticles in the composites.

4.3. Low velocity impact

The impact behavior of all epoxy nanocomposite laminate was evaluated. The results were repeatable for all the three specimens tested under the same conditions. The graphs presented are averages of the specimens for each sample. To eliminate the noise of the test which is inherent to the experiment, and also to allow for easier comparison between graphs of different nanocomposites, a moving average of each result was calculated and illustrated.

4.3.1. Force-time responses

Fig. 3 shows the force-time (F-t) curves of all the GO, rGO and GNPs laminates at different concentrations of nanoparticles. In these graphs, force curves decrease to zero after the duration of contact which is an indication that the specimen was not penetrated under impact. The F-t curves are characterized by an ascending section of loading, a section of reaching a maximum force value (named peak load – P_m, see Fig. 3) and a descending part of unloading. The descending part of the intact profile of the load-time graph shows fluctuations in load which is generally indicative of delamination. According to the force-time curves of GO-modified composites (Fig. 3a), unlike neat epoxy plate that showed a drop in force (i.e. delamination), the nanocomposite samples with GO 1

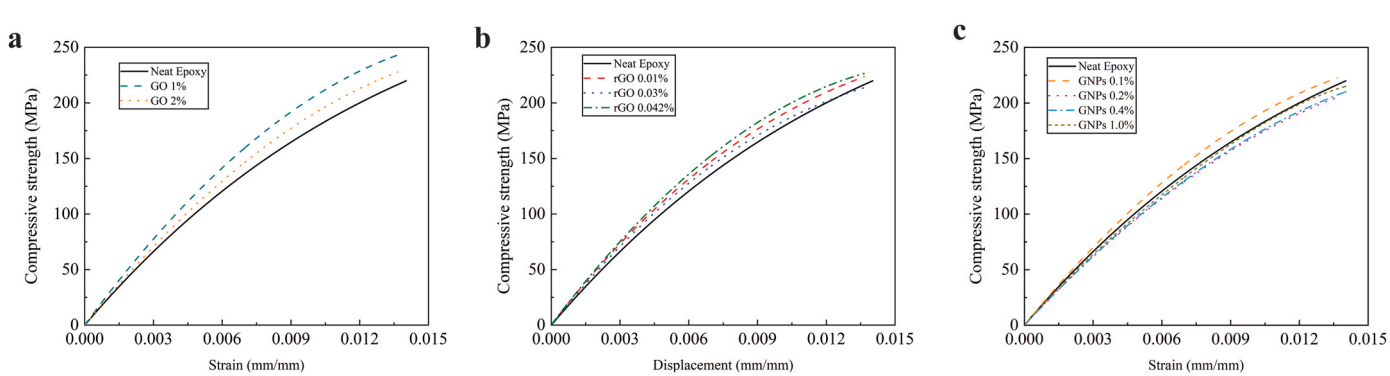

Fig. 2. The compression stress–strain curves for the glass–epoxy composites including nanoparticles of a) GO, b) rGO and c) GNPs.

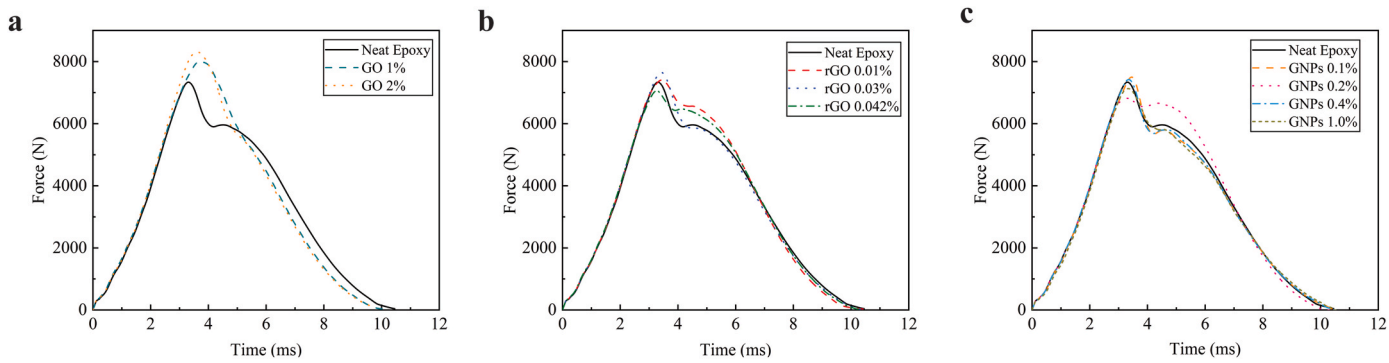

Fig. 3. Load-time (F-t) curves of all the a) GO, b) rGO and c) GNPs laminates at different concentrations of the nanoparticles.

% and 2 % showed no fluctuation which suggested that the introduction of GO was effective in strengthening the composites against delamination. The GO-modified composites also yielded a higher maximum force values which was another sign that GO-modified plates have more strength against drop weight impact. The enhanced impact resistance can be attributed to the strong interfacial bonding between the graphene oxide and the epoxy matrix, which helps distribute impact energy more evenly and suppresses the initiation and propagation of delamination and matrix cracks. A similar improvement was also found in nanocomposites modified with rGO (Fig. 3b); however, in the case of GNPs, only 0.1 wt% loading of GNPs led to improvement in force-time history curves (i.e. better impact resistance) and higher loading of GNPs were inferior to neat epoxy samples. Similar to the case of compression, agglomeration of graphene layers at higher contents is expected to be the reason for this. The highest P_m among all the samples belonged to those composites containing GO nanoparticles. The percentage increase

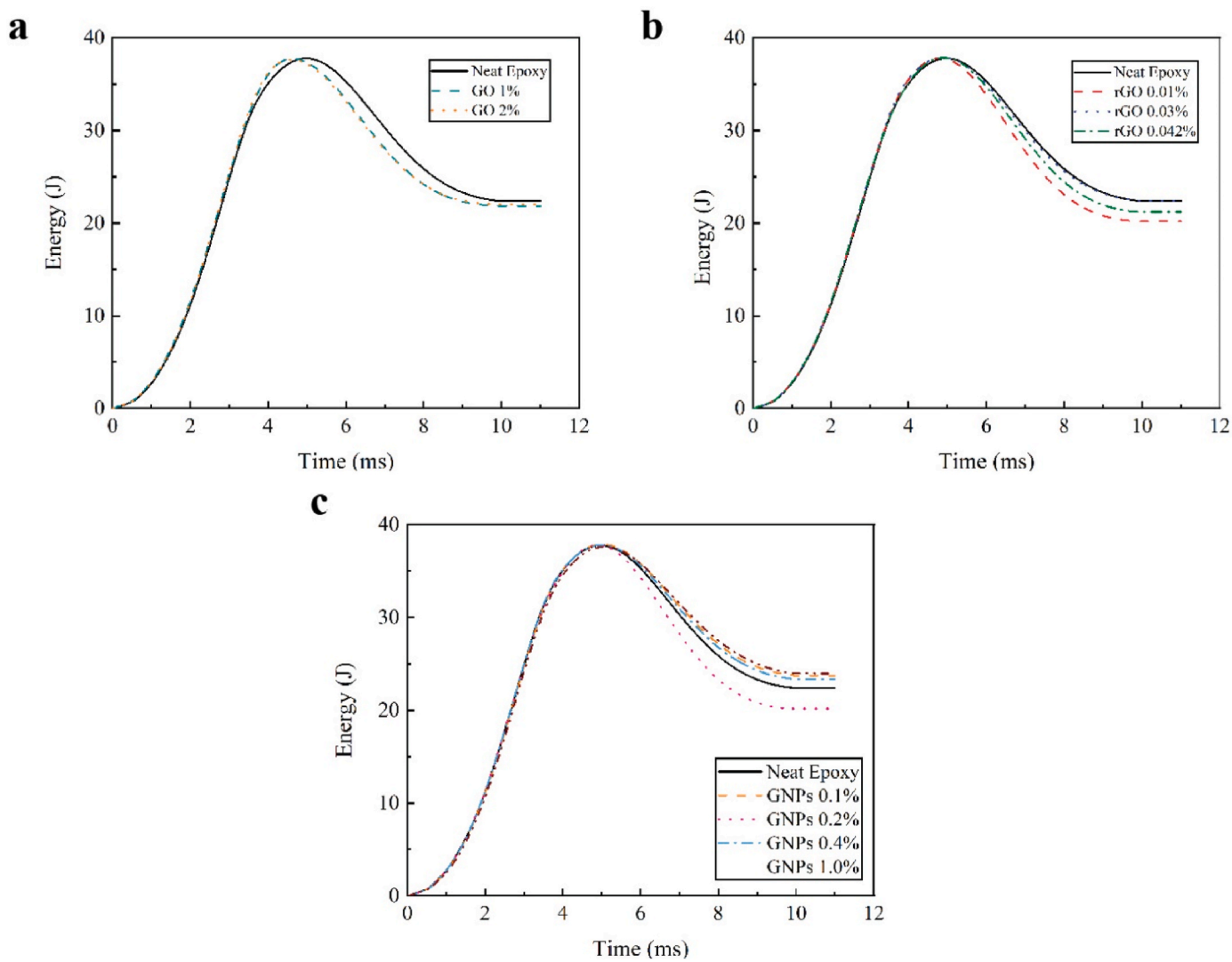

Fig. 4. Energy-time curves of multiscale composites modified with a) GO, b) rGO and c) GNPs at different concentrations of the nanoparticles.

of P_m for these samples were 8.9 and 13.1 % for the samples containing 1 and 2 wt % of the GO nanoparticles, respectively.

4.3.2. Energy-time responses

The absorbed energy, E_a, with respect to time t was expressed using the following equation given in ASTM D7136:

$$E_a(t) = \frac{m(v_i^2 - v(t)^2)}{2} + mg\delta(t) \quad (1)$$

where m is the mass of the impactor, v_i is the impact velocity, v is the impactor velocity at time t, g is the acceleration due to gravity, and δ is the deflection at time t. Eq. (1) is plotted in Fig. 4, with respect to time. During service use, material panels under impact may not completely fracture and may or may not show any sign of damage on the surface. In this case, slight surface damage was observed, and a loss of absorbed energy due to localized material failure is evidenced in Fig. 4, where the absorbed energy levels off at a value of 22.4 J in the case of NE (Neat Epoxy). This value was lower in the case nanocomposites contacting rGO nanoparticles, (20.2, 21.2 and 22.4 J for 0.01, 0.03 and 0.042 wt % respectively) and GO nanoparticle (22.03 J and 21.86 J for 2 and 1 wt % respectively) and higher for most GNPs loadings (23.75, 20.17, 23.34, and 23.96 J for 0.1, 0.2, 0.4 and 1 wt % respectively). As shown in the diagram, the impactor velocity reached zero, and the kinetic energy of the impactor was transferred to the structure completely. In a plate recovery process, the kinetic energy of the plate reaches a constant level following the damage caused by structural and frictional factors.

4.3.3. Force-displacement responses

Impact force vs penetration displacement of the impactor for neat epoxy and its nanofilled composites and the slope of the elastic force-displacement regime (flexural stiffness) are plotted in Fig. 5., allowing for a comparison of stiffnesses of the laminates during the impact test. Indeed. the slope of the moving average of the force-deflection curves is directly related to the impact bending stiffness. Among all the samples studied, the nanocomposites reinforced with GO with a weight percentage of 1 wt % and 2 wt % had the highest bending stiffness. The addition of rGOs also resulted in increasing the stiffness of the composite panel. However, GNPs did not appear to be as effective as GO and rGo in improving the stiffness of laminates. From Fig. 5, it is also apparent that samples containing GO and rGO nanoparticles outperformed the neat epoxy when it came to deflection. The reduced deflection was an indication of the composite resistance to delamination. Therefore, among the nanofillers studied, it can be stated that GO was the most effective in this regard.

4.4. Residual strength after impact

The impact specimens were tested in compression to investigate the residual compression strength (CAI tests). These tests are complicated and the results strongly depend on the quality of the laminate. Some of the cracks and imperfections caused during impact tests led to incorrect failures and, therefore, to an incorrect residual strength evaluation. Unfortunately, a large number of tests gave nonacceptable results. Thus, the results discussed in this section are for the sample which successfully passed the test.

The compressive properties measured in this test were significantly influenced by the type, orientation, and volume fraction of fibers, as well as their interfacial bonding with the polymer matrix. The stress–strain curves for the undamaged (Fig. 2) and damaged (Fig. 6) nanocomposite laminates exhibited similar elastic regions, indicating that the fibers carried the majority of the applied load. This consistent behavior highlights the critical role of fibers in resisting compressive stresses. However, notable differences were observed in the ultimate strength and strain values between the undamaged and damaged samples, reflecting variations in their structural integrity and internal soundness (see Table 4). The undamaged composite samples demonstrated the highest compressive strength due to their nearly flawless internal structure, which ensured efficient load transfer and resistance to failure. In contrast, the damaged laminates exhibited significantly lower compressive strength, primarily due to the presence of internal cracks and damaged fibers caused by prior low-velocity impact. These defects compromised the load-bearing capacity and introduced stress concentration points, accelerating failure. As shown in Fig. 6, composites modified with graphene oxide (GO) consistently outperformed the neat epoxy samples. This aligns with the results from the undamaged compressive tests, where GO-enhanced composites demonstrated superior performance. The improved compressive behavior of GO-modified laminates is attributed to the strong interfacial bonding between GO and the polymer matrix, which helps to distribute stress more evenly and reduce the propagation of cracks and delamination under compressive loads. Occasionally, there were some mismatched trends between damaged and undamaged composite samples, mainly for some of the rGO and GNP modified samples. This might be due to some variations in the impacted area of damaged samples.

Although it was observed that the compressive strength was affected by the impact damage, all the nanocomposite samples had higher CAI ultimate strength and strain values compared to the neat epoxy composites, these improvements were mostly negligible. The compressive modulus after the impact of damaged specimen was generally much lower than those of their undamaged counterparts. Within the CAI group of specimens, the GO composites revealed higher compressive modulus than the neat epoxy controls. However, this trend was not observed in rGO and GNP composites. Similar to the case of CAI stress-strain curves, this might be due to some variations in the impacted area of damaged samples.

5. Conclusion

Three different types of nanofillers, GO, rGO and GNP were used as

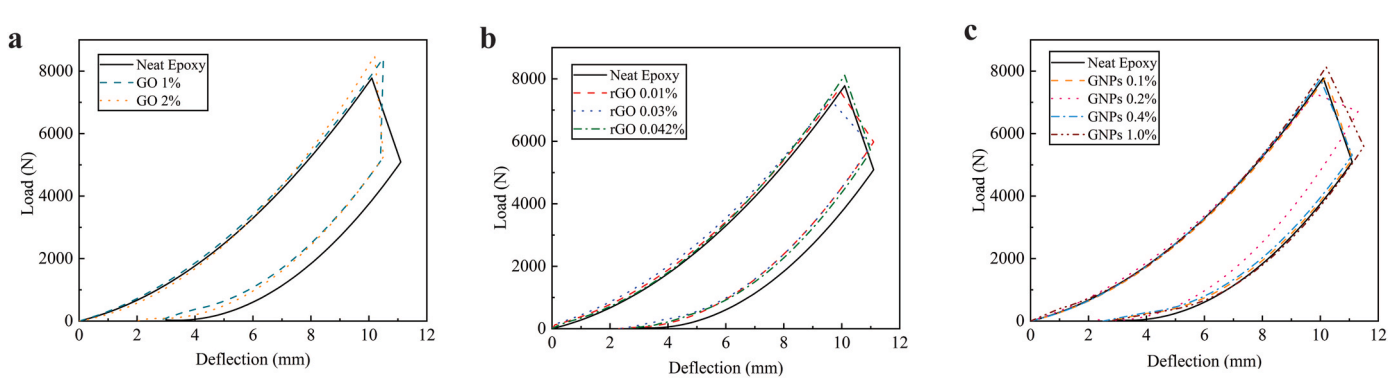

Fig. 5. Force-displacement curves of multiscale composites modified with a) GO, b) rGO and c) GNPs at different concentrations of the nanoparticles.

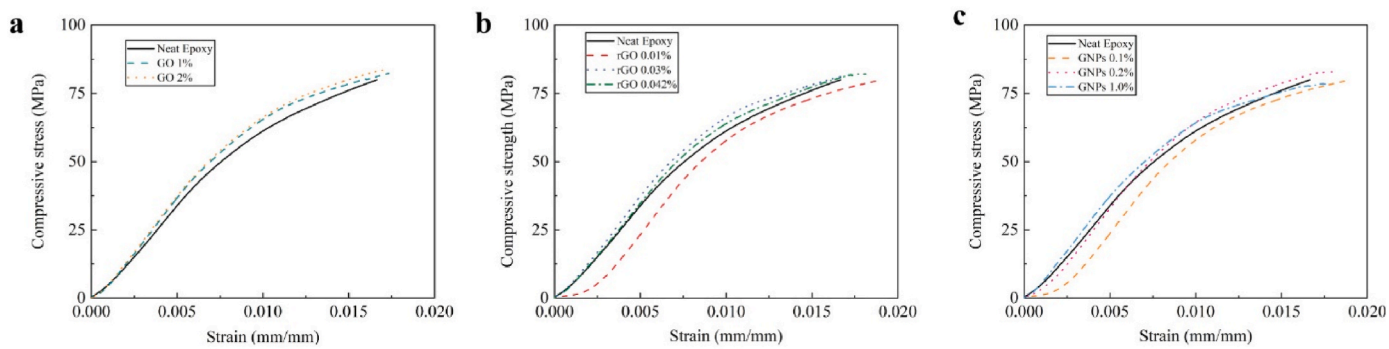

Fig. 6. The stress–strain curves of compression test for damaged composite of nanocomposites containing a) GO, b) rGO and c) GNPs.

Table 4
Quantified results for compression after impact tests: Compressive modulus, Maximum compressive strength and maximum compressive strength of nanocomposites containing GO, rGO and GNPs.

Case	Compressive modulus (GPa)		Ultimate compressive strain		Ultimate compressive strength (MPa)	
	Average	STD Dev.	Average	STD Dev.	Average	STD Dev.
Neat Epoxy	6.8	0.8	8.06E-04	2.05E-04	75.5	6.3
GO 1 %	7.9	0.5	8.28E-04	5.50E-05	83.1	3.0
GO 2 %	7.8	0.2	8.38E-04	4.40E-05	81.2	1.7
rGO 0.01 %	3.5	1.8	9.18E-04	7.54E-05	79.7	2.4
rGO 0.03 %	7.6	0.6	8.18E-04	2.58E-05	81.2	0.3
rGO 0.042 %	7.2	0.1	8.82E-04	2.47E-05	82.4	1.1
GNPs 0.1 %	4.2	0.9	9.20E-04	7.24E-05	79.7	2.4
GNPs 0.2 %	5.6	1.4	8.86E-04	3.29E-05	83.6	1.5
GNPs 1.0 %	8.0	0.1	8.45E-04	3.21E-05	78.4	0.8

reinforcement agents to tentatively improve the mechanical properties (particularly compressive behavior) in fiber/glass epoxy nanocomposites. A multiscale laminated nanocomposite of fiberglass/epoxy was prepared using the VARTM method. An investigation of the mechanical properties of glass fiber-reinforced multiscale composites was then conducted. For the compression test, it was observed that for all configurations containing GO and rGO, the measured compressive strength was higher than those of the neat fiber/epoxy ones. However, in the case of GNPs, adding 0.1 wt% of GNPs improved the compressive strength that it has nearly 0.012 increased by percent, while a further increase in GNPs reduced the compressive properties. Agglomeration of graphene layers at higher contents is expected to be the reason for this decrease. In other cases, they have changed almost negligibly. A similar trend was observed for the compressive moduli. According to the force-time curves of GO-modified composites in low velocity impact tests, unlike neat epoxy plates that showed a drop in force (i.e. delamination), the nanocomposite samples with GO 1 % and 2 % showed no fluctuation, but in the GO 2 % case, which it has shown an increase of about 13 % that introduction of GO was effective in strengthening the composites against delamination. The carbon-nanomaterials modified composites also generally yielded a higher maximum force values which was another sign that carbon-nanomaterials modified plates had generally more strength against drop weight impact. Residual strength after impact tests showed that although the compressive strength was affected by the impact damage, all the nanocomposite samples had higher CAI ultimate strength and strain values compared to the neat epoxy composites. Nevertheless, these improvements were mostly statistically insignificant.

CRediT authorship contribution statement

M. Rafiee: Writing – original draft, Methodology, Investigation, Data curation, Conceptualization. **A. Fallah:** Writing – review & editing, Writing – original draft, Software, Data curation. **S. Hosseini Rad:** Writing – original draft, Methodology, Investigation, Data curation. **M. R. Labrosse:** Supervision, Project administration, Funding acquisition.

Data availability

The raw data for reproducing these findings are available upon request.

Declaration of competing interest

The authors declare that they have no known competing financial interests or personal relationships that could have appeared to influence the work reported in this paper.

References

[1] M. Rafiee, F. Nitzsche, M. Labrosse, Effect of functionalization of carbon nanotubes on vibration and damping characteristics of epoxy nanocomposites, Polym. Test. 69 (2018) 385–395.
[2] M. Rafiee, F. Nitzsche, M.R. Labrosse, Cross-sectional design and analysis of multiscale carbon nanotubes-reinforced composite beams and blades, International Journal of Applied Mechanics 10 (3) (2018 Apr 26) 1850032.
[3] W. Xin, et al., Impact and post-impact properties of multiscale carbon fiber composites interleaved with carbon nanotube sheets, Compos. B Eng. 183 (2020) 107711.
[4] A. Pandian, et al., Low Velocity Impact Studies on Fibre-Reinforced Polymer Composites and Their Hybrids–Review, 2020.
[5] S. Liu, et al., A review of extending performance of epoxy resins using carbon nanomaterials, Compos. B Eng. 136 (2018) 197–214.
[6] M. Quaresimin, et al., Toughening mechanisms in polymer nanocomposites: from experiments to modelling, Compos. Sci. Technol. 123 (2016) 187–204.
[7] R. Eslami-Farsani, et al., Recent trend in developing advanced fiber metal laminates reinforced with nanoparticles: a review study, J. Ind. Textil. 51 (5_suppl) (2022) 7374S–7408S.
[8] L. Guo, et al., Advances and outlook in modified graphene oxide (GO)/epoxy composites for mechanical applications, Appl. Nanosci. 13 (5) (2023) 3273–3287.
[9] M. Rafiee, F. Nitzsche, M.R. Labrosse, Processing, manufacturing, and characterization of vibration damping in epoxy composites modified with graphene nanoplatelets, Polym. Compos. 40 (10) (2019) 3914–3922.
[10] M. Sieradzka, et al., A facile approach to obtaining PVDF/graphene fibers and the effect of nanoadditive on the structure and properties of nanocomposites, Polym. Test. 81 (2020) 106229.
[11] L.G. Amurin, et al., Multifunctionality in ultra high molecular weight polyethylene nanocomposites with reduced graphene oxide: Hardness, impact and tribological properties, Polymer 240 (2022) 124475.
[12] X. Huang, et al., Thermal conductivity of graphene-based polymer nanocomposites, Mater. Sci. Eng. R Rep. 142 (2020) 100577.

[13] C.V. Katsiropoulos, et al., Enhancement of damping response in polymers and composites by the addition of graphene nanoplatelets, Compos. Sci. Technol. 227 (2022) 109562.
[14] Q. Yan, et al., Improved mechanical properties in titanium matrix composites reinforced with quasi-continuously networked graphene nanosheets and in-situ formed carbides, J. Mater. Sci. Technol. 96 (2022) 85–93.
[15] S. Shanmugam, O. Meenakshisundaram, Experimental investigation of graphene filled flax/E-glass/epoxy hybrid nanocomposites on physical, mechanical, and thermal properties, Fullerenes, Nanotub. Carbon Nanostruct. 31 (1) (2023) 38–50.
[16] M.V. Çakır, A. Erkliğ, B.F. Ahmed, Graphene nanoparticle effect on flexural and shear behaviors of adhesively bonded single lap joints of GFRP composites, J. Braz. Soc. Mech. Sci. Eng. 43 (2021) 1–11.
[17] N. Nash, et al., Inclusion of a thermoplastic phase to improve impact and post-impact performances of carbon fibre reinforced thermosetting composites—a review, Mater. Des. 85 (2015) 582–597.
[18] N.F. Doğan, et al., Mechanical and low velocity impact characterization of carbon/glass hybrid composites with graphene nanoplatelets, Mater. Res. Express 6 (8) (2019) 085304.
[19] N.F. Doğan, Ö. Özbek, A. Erkliğ, Effect of graphene nanoplatelets on mechanical and impact properties of an aramid/glass-reinforced epoxy composite, Mater. Test. 64 (4) (2022) 490–501.
[20] A.S. Rahman, V. Mathur, R. Asmatulu, Effect of nanoclay and graphene inclusions on the low-velocity impact resistance of Kevlar-epoxy laminated composites, Compos. Struct. 187 (2018) 481–488.
[21] M. Rezvani Tavakol, et al., Effect of graphene nanoparticles on the strength of sandwich structure inspired by dragonfly wings under low-velocity impact, Polym. Compos. 42 (10) (2021) 5249–5264.
[22] G. Vigneshwaran, et al., Tensile, impact, and mode-I behaviour of glass fiber-reinforced polymer composite modified by graphene nanoplatelets, Arch. Civ. Mech. Eng. 20 (2020) 1–15.
[23] M.T. Demirci, Investigation of low-velocity impact behavior of aluminum honeycomb composite sandwiches with GNPs doped BFR laminated face-sheets and interfacial adhesive for aircraft structures, Polym. Compos. 43 (8) (2022) 5675–5689.
[24] A. Fathi, G. Liaghat, H. Sabouri, An experimental investigation on the effect of incorporating graphene nanoplatelets on the low-velocity impact behavior of fiber metal laminates, Thin-Walled Struct. 167 (2021) 108162.
[25] M. Rafiee, et al., Simultaneous reinforcement of matrix and fibers for enhancement of mechanical properties of graphene-modified laminated composites, Polym. Compos. 40 (S2) (2019) E1732–E1745.
[26] M. Rafiee, et al., Thermal properties of doubly reinforced fiberglass/epoxy composites with graphene nanoplatelets, graphene oxide and reduced-graphene oxide, Compos. B Eng. 164 (2019) 1–9.
[27] K.-t. Lau, C. Gu, D. Hui, A critical review on nanotube and nanotube/nanoclay related polymer composite materials, Compos. B Eng. 37 (6) (2006) 425–436.
[28] B. Zhang, et al., Mechanical and thermal properties of hierarchical composites enhanced by pristine graphene and graphene oxide nanoinclusions, J. Appl. Polym. Sci. 131 (19) (2014).